JOURNAL OF AGRICULTURAL AND FOOD CHEMISTRY
ARTICLE

J. Agric. Food Chem. 2009, 57, 6927–6931 6927
DOI:10.1021/jf9016459

Separation of Phthalocyanine-like Substances from Humic Acids Using a Molecular Imprinting Method and Their Photochemical Activity under Simulated Sunlight Irradiation

Chunyan Yu,[†] Shuo Chen,[†] Xie Quan,*[,†] Xiaoxia Ou,[‡] and Yaobin Zhang[†]

[†]Key Laboratory of Industrial Ecology and Environmental Engineering (Ministry of Education, China), School of Environmental and Biological Science and Technology, Dalian University of Technology, Dalian 116024, China, and [‡]College of Life Science, Dalian Nationalities University, Dalian 116605, China

To elucidate the existence of phthalocyanine-like (*Pc*-like) substances in humic acids (HA) and their roles in photochemical transformation of organic pollutants, *Pc*-imprinted polymers (MIP) were synthesized successfully and employed to separate *Pc*-like substances from HA. The fraction bound by MIP ($F_{mip\text{-}b}$) presented better photochemical activity for degradation of 2,4-dichlorophenoxyacetic acid (2,4-D) in aqueous solution irradiated by simulated sunlight. The pseudo-first-order rate constant of 2,4-D photodegradation with the presence of $F_{mip\text{-}b}$ was 2.5 times as high as that in solution containing effluent fraction (F_{eff}). These results show the key role of some HA with special structures in photochemistry and are helpful for better understanding phototransformation of environmental contaminants in natural aquatic systems.

KEYWORDS: Humic acids; molecularly imprinted polymers; phthalocyanine; photodegradation; 2,4-dichlorophenoxyacetic acid

INTRODUCTION

Humic acids (HA), the major components of dissolved organic matter (DOM), are widely distributed in nature. In the aquatic environment, HA plays an important role in photochemistry because it is one of the most important natural sunlight-absorbing components. Photochemical processes involving HA often yield reactive oxygen species (ROS), which can affect the transfer and transformation of persistent toxic substances (PTS) in natural water under sunlight irradiation (*1*). Numerous studies have demonstrated that the existence of HA in water could enhance the photodegradation of coexisting PTS (*2*, *3*), whereas other researchers found that HA could inhibit the photodegradation of other substances (*1*). The enhancement or retardation was assumed to depend on the origins of the HA, their concentrations, and experimental conditions (*4*). Molecular structures of different substances in HA might be key factors influencing their photochemical behavior. It is well-known that chlorophyll in plants plays a key role during their living period. Under sunlight irradiation, chlorophyll might result in a series of electron transfer steps due to the presence of extended π-conjugated structure, and thus it could affect the transfer and transformation of other coexisting organic compounds. After their life cycle finishes, plants gradually decompose and become smaller organic substances (humic substances) through humification (*5*). Some basic chemical units or groups in the original plants would remain in humic substances. Therefore, it is reasonable to expect that chlorophyll-like structures might exist in humic substances. However, because of the difficulty in separating the substances with specific structures, the relationship between photochemical activity and HA structure has not been well established, although some researchers have reported some interesting findings that photochemical activity of HA is related to molecular weight (*6*, *7*). Separation of HA according to structure speciation and recognition of the structures with specific photoactivity are potentially helpful for better understanding phototransformation of environmental contaminants in natural aquatic systems.

Various techniques, such as chromatographic techniques, ultrafiltration, capillary electrophoresis, and flow field flow fractionation, have been developed to separate HA (*8*). These methods could mainly classify HA in terms of either molecular size or polarity. However, they are not suitable for HA separation in terms of structure recognition. Recently, molecular imprinting, as a separation technique, has been extensively studied. The molecular imprinting systems are usually created by imprinting template molecules in a rigid porous polymers matrix through the non-covalent/covalent interactions between template molecule and functional monomer (*9*). After removal of the templates, the resulting polymers contain recognition sites (cavities) that are complementary in shape and functionality to the template molecules (*10*). Molecularly imprinted polymers (MIP) have been widely applied in separation, sensors, synthesis, and catalysis (*11*, *12*). The unique ability of the MIP technique in molecular recognition and binding makes it possible to separate HA in accordance with molecular structure characters.

The main objective of this work was to recognize and separate the substances with chlorophyll-like structures from HA and evaluate their photochemical activity in degradation of PTS. A MIP solid phase extraction (MIP-SPE) cartridge was prepared for the separation of desired structures from HA. Because

*Corresponding author (telephone +86-411-84706140; fax +86-411-84706263; e-mail quanxie@dlut.edu.cn).

Published on Web 07/10/2009

chlorophyll is not chemically stable (*13*) in the process for MIP preparation, phthalocyanine (*Pc*), which has extended π-conjugated structure and photochemical property similar to those of chlorophyll (*14*, *15*) (Figure S1 of the Supporting Information), was employed in the MIP as template molecule. Additionally, *Pc* is widely distributed in nature and possesses higher thermal and chemical stability (*15*, *16*) than chlorophyll. Recently, *Pc* has been extensively studied in solar cells, color sensor, and photocatalysis (*15*). To evaluate the photochemical activity of the HA fractions, a widely used herbicide, 2,4-dichlorophenoxyacetic acid (2,4-D), which is a suspected endocrine disruptor and a possible human carcinogen, as a kind of PTS often detected in ground and surface waters (*17*, *18*), was selected as a probe compound in the photodegradation experiment.

MATERIALS AND METHODS

Chemicals. α-Methacrylic acid (MAA) and 2,2′-azobis(isobutyronitrile) (AIBN) were purchased from Damao Chemistry Reagent Co. and Fuchen Chemistry Reagent Co. (Tianjin, China), respectively. Ethylene glycol dimethacrylate (EGDMA) was supplied by Alfa Aesar, A Johnson Matthey Co. (Ward Hill, MA). Copper phthalocyanine (CuPc) and 5,5-dimethyl-1-pyrroline-*N*-oxide (DMPO) were obtained from Tokyo Chemical Industry Co., Ltd. (Japan). Oxalic acid, citric acid, salicylic acid, glucose, and sucrose were obtained from Bodi Chemistry Reagent Co. (Tianjin, China). All chemicals were of analytical reagent grade and used as received. HA originated from soil was supplied by MP Biomedicals, Inc. (Eschwege, Germany). Stock solution of HA was prepared in Milli-Q water, and the pH of the HA solution was adjusted to 8.5 by 0.1 mol L^{-1} NaOH. The concentration was measured by a total organic carbon analyzer (TOC-V_{CPH}, Shimadzu, Japan). 2,4-D (purity > 98%) was purchased from Labor Dr. Ehrenstorfer (Augsburg, Germany). Stock solution of 2,4-D (500 mg L^{-1}) was prepared in methanol and stored in a refrigerator at 4 °C in dark.

Characterization. Ultraviolet−visible (UV−vis) absorbance spectra of liquid and solid samples were measured with a UV−vis spectrophotometer (UV-550, Jasco, Japan) and a UV−vis diffuse reflectance spectrophotometer (DRS, UV-2450, Shimadzu, Japan), respectively. Fourier transform infrared spectroscopy (FTIR) was used to analyze functional groups in HA and recorded with an FTIR spectrometer (Prestige-21, Shimadzu, Japan). Brunauer−Emmett−Teller (BET) surface area was measured using nitrogen adsorption analyzer (Autosorb-1, Micromeritics Instrument Corp., Norcross, GA). The fluorescence of HA was measured using a fluorescence spectrophotometer (model F-4500, Hitachi, Japan). Electron paramagnetic resonance (EPR) measurements were performed using a Bruker model EPR 300E spectrometer equipped with a Quanta-Ray Nd: YAG laser (λ = 355 nm), and DMPO was used as the spin-trapper for trapping radicals. To minimize experimental errors, the same quartz capillary tube was used for all EPR measurements.

Preparation of MIP. The template molecule, functional monomer, cross-linking agent, and initiator used in this study were CuPc, MAA, EGDMA, and AIBN, respectively. CuPc (1 mmol), MAA (4 mmol), EGDMA (20 mmol), and AIBN (40 mg) were dissolved in chloroform (12 mL) in a glass tube. The mixture solution was sonicated for 5 min, flushed with nitrogen gas for 15 min, and then polymerized by heating at 60 °C in a thermostatic water bath for 24 h. The obtained blue solid polymers (MIP) were ground and sieved. To remove the template molecules, the polymers were washed with methanol/acetic acid (9:1, v/v) in an incubating shaker at 30 °C until no template molecules were detected in the eluant with the UV−vis spectrophotometer. As a control, nonimprinted polymers (NIP) were prepared in the same manner only without CuPc template. MIP and NIP were dried and used for binding experiments.

MIP-SPE Cartridges Preparation and Binding Experiments. MIP (0.25 g) was placed into an empty polytetrafluoroethylene (PTFE) solid phase extraction (SPE) cartridge (6 mL) to prepare the MIP-SPE cartridge. PTFE frits were placed above and below the sorbent bed. As a control, a column with NIP (NIP-SPE) was also prepared in the same manner.

Twenty milliliters of CuPc (dissolved in chloroform) solution was passed through the MIP-SPE cartridge at a flow rate of 0.5 mL min^{-1}, and then the solid polymers were collected and dried. The rebinding CuPc capability of MIP was investigated by measuring the difference between the amount of CuPc in polymers before and after binding CuPc. The polymers were analyzed by DRS. In addition, oxalic acid, citric acid, glucose, and sucrose solutions were prepared in Milli-Q water, and salicylic acid was prepared in ethanol. These solutions were passed through the MIP-SPE cartridge at a flow rate of 0.5 mL min^{-1}, and then the eluants were collected, respectively. The selectivity of MIP was investigated by measuring the difference between the initial and eluted concentrations of solutions. All solutions were analyzed using a UV−vis spectrophotometer.

Fractionation Procedure of HA by MIP. Prepared MIP is used for selectively retaining a fraction that has a structure similar to that of *Pc* in HA. Twenty milliliters of HA aqueous solution (5 mg L^{-1}) passed through the MIP-SPE cartridge at a flow rate of 0.5 mL min^{-1}. The effluent fraction was collected and named F_{eff}. The bound fraction was washed using 60 mL of fresh Milli-Q water and collected (F_{mip-b}). Both fractions were concentrated to the desired concentration through evaporation at 60 °C in a thermostatic water bath and used for photochemical experiments. It was estimated on the basis of mass balance calculation that F_{mip-b} was about 2% in the HA.

Photochemical Experiments and Chemical Analysis. One hundred and twenty milliliters aqueous solutions containing 1 mg L^{-1} 2,4-D and 5, 15, or 45 mg L^{-1} HA fractions were put into quartz tubes with stopper. The quartz tubes were placed in a phytotron chamber equipped with three 1800 W Xe lamps with special glass filters restricting the transmission of wavelengths below 290 nm to simulate sunlight. Experiments were performed under an irradiation intensity of 12 mW cm^{-2} and a temperature of 21 ± 1 °C. Milli-Q water was used in the photochemical experiments. The pH for all solutions remained about 6.2 and was not adjusted.

The concentration of 2,4-D was analyzed by high-performance liquid chromatography (HPLC, Waters 2695, photodiode array detector (PDA)-2996, Waters, Milford, MA), equipped with a SunFire ODS reverse-phase column (4.6 × 150 mm, 5.0 μm). The external standard method was selected in the study. A mixture of methanol and 0.2% of phosphoric acid solution (v/v, 65:35) was used as the mobile phase at a constant flow rate of 1.0 mL min^{-1}. The detector wavelength was set at 230 nm.

RESULTS AND DISCUSSION

Characterization of Polymers. CuPc is composed of a central Cu atom surrounded by four pyrrole rings that are attached to benzene rings and are bridged by four additional N atoms (*19*), which could form hydrogen bonds with functional monomers. FTIR spectra were used to study intermolecular hydrogen bond interactions between template molecule CuPc and functional monomer MAA in MIP before template molecule CuPc removal. **Figure 1** shows a small band at 1510 cm^{-1} in MIP, possibly ascribed to C═C stretching of aromatic rings and conjugated C═N systems (*20*, *21*), due to the presence of CuPc. The strong peaks at 3700−3200 cm^{-1} in all spectra could be attributed to the presence of −OH stretch in MAA. Before elution, MIP and NIP exhibited characteristic peaks of a −OH group at 3415 and 3523 cm^{-1}, respectively. Compared with the infrared data of NIP, the −OH stretching vibrational frequency of MIP shifted to a lower frequency, indicating CuPc binds with MAA through −OH···N hydrogen bonds. Figure S2 of the Supporting Information shows the molecular imprinting process and the formation of hydrogen bonds.

MIP is a class of network materials known as microporous polymers (*10*). Comparison of surface areas and porosities of MIP before and after removal of template could indicate whether the template was removed from the polymers effectively. To observe surface states of the polymers, surface areas and porosities were analyzed by nitrogen adsorption analyzer. BET surface areas of MIP before and after elution were 204 and 225 m^2 g^{-1} and their pore sizes were 9.89 and 8.74 nm, respectively. Because the template molecules and the unpolymerized residues were

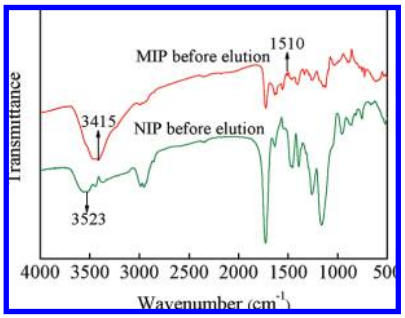

Figure 1. FTIR spectra of imprinted polymers (MIP) and nonimprinted polymers (NIP) before elution.

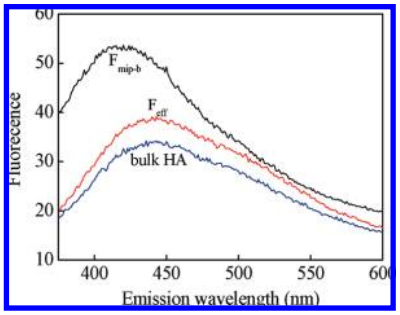

Figure 2. Fluorescence emission spectra of HA and its fractions with TOC concentration of 5 mg L^{-1}. Excitation wavelength = 320 nm.

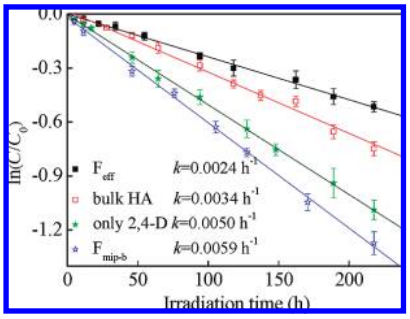

Figure 3. First-order rate constants (k) calculated at different HA fractions with TOC concentration of 5 mg L^{-1} on 2,4-D (1 mg L^{-1}) degradation.

removed with methanol/acetic acid (9:1, v/v), the eluted MIP had more pores of different sizes. As a result, the MIP after elution exhibited slightly higher surface areas but lower average pore sizes than before, implying that template molecules and the unpolymerized residues were removed efficiently.

Rebinding Capability and Selectivity of MIP. The molecular recognition property of MIP was evaluated by comparing binding amount of template molecules between MIP and NIP. Figure S3a of the Supporting Information shows UV−vis DRS spectra of MIP and NIP before and after binding CuPc. According to the calibration curve for CuPc (data not shown) based on DRS measurement, it was calculated that 8.75 and 1.80 mg of CuPc were adsorbed by 0.25 g of MIP and NIP, respectively. The almost 4 times greater binding amount on MIP than on NIP illustrates that MIP has high *Pc* recognition capability and, thus, exhibits high selectivity for *Pc* binding. The increment of effective recognition sites is mainly attributed to strong non-covalent interaction between CuPc molecules and MAA, the −OH of which can interact with N atoms of CuPc molecules to form hydrogen bonds. The CuPc retention on NIP relied on nonspecific adsorption to a large extent. The results revealed that the formation of binding sites with higher affinity for the template molecules led to higher rebinding capability of MIP to CuPc than that of NIP.

To further elucidate the capability for selective binding of *Pc*-like substances from HA for the prepared MIP, batch binding tests for some elementary structures in HA, such as oxalic acid, citric acid, salicylic acid, glucose, and sucrose onto MIP-SPE, were investigated. Because there are −COOH or −OH groups in these substances, it is possible to form hydrogen bonds for the substances with MIP. The chemical structures of these substances are shown in Figure S4 of the Supporting Information. UV−vis measurement was applied to determine the concentrations of either original solutions or effluents from MIP-SPE or NIP-SPE cartridges. Figure S3b−f of the Supporting Information shows that differences of absorbance between original solutions and effluents for all five tested substances were negligible. This means that these substances did not effectively bind onto either MIP or NIP. These results demonstrated that MIP possessed high selectivity and thus only the structures similar to *Pc* in HA could be bound by MIP.

Fluorescence of HA and Its Fractions. HA is known to be fluorescent. Fluorescence properties have been often used to characterize and/or to discriminate HA of different origins, naturally occurring organic matter, and humic-like materials extracted from composts (*22*). The substances with more fluorophores could display better photoinductive activity (*7*). The fluorescence emission maximum depended on the chosen excitation wavelength (*23*). According to the three-dimensional excitation/emission matrix spectra of different HA fractions and bulk HA (data not shown), the excitation wavelength was set at 320 nm, and the emission wavelength ranged from 330 to 600 nm. Their fluorescence emission spectra are given in **Figure 2**. Concentrations of each fraction and bulk HA were 5 mg L^{-1}. All three samples exhibited broad emission bands, but $F_{mip\text{-}b}$ showed a slightly narrow curve shape with a maximum intensity around 417 nm, whereas similar curve shapes with a maximum intensity around 442 nm were observed for both F_{eff} and bulk HA. The fluorescence intensity of $F_{mip\text{-}b}$ was obviously greater than that of F_{eff} and bulk HA. It was attributed to the *Pc*-like structures in $F_{mip\text{-}b}$ involving the strong π-conjugated system, which is well-known to induce fluorescence. F_{eff} gave slightly more intense fluorescence than bulk HA. The reason is not clear and needs further investigation. Possibly, the fluorescence of bulk HA decreases as a result of the intermolecular interactions between *Pc*-like substances and other substances, which could cause a shielding effect and reduction of fluorophores involved in HA (*24*).

Effects of HA and Its Fractions on 2,4-D Photodegradation. To observe the photochemical behavior of different HA fractions, the photodegradations of 2,4-D (initially 1 mg L^{-1}) in solutions containing different HA fractions and bulk HA (initially 5 mg L^{-1}) were investigated under simulated solar light irradiation ($\lambda >$ 290 nm), and the results are shown in **Figure 3**. In the dark control experiment (data not shown), no obvious changes of 2,4-D concentration were observed in the solution during the 233 h experimental period, indicating no other significant transformation reaction over the time scale considered. Under simulated sunlight irradiation, difference in the 2,4-D degradation was observed. Degradation rates of 2,4-D photodegradation varied in the following order: presence of $F_{mip\text{-}b}$ > without any HA or its fractions > bulk HA > F_{eff}. The 2,4-D photodegradations in the study were found to fit the pseudo-first-order reaction kinetics, and the apparent first-order rate constant k was estimated according to equation $\ln(C/C_0) = -kt$, where C represents 2,4-D

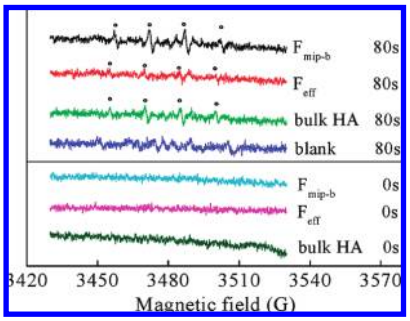

Figure 4. EPR signals of the DMPO−OH• adduct in solutions of HA and its fractions with TOC concentration of 32 mg L^{-1}. The signals were recorded in the dark (0 s) and at $\lambda = 355$ nm irradiation (80 s) [DMPO] = 80 mmol L^{-1}.

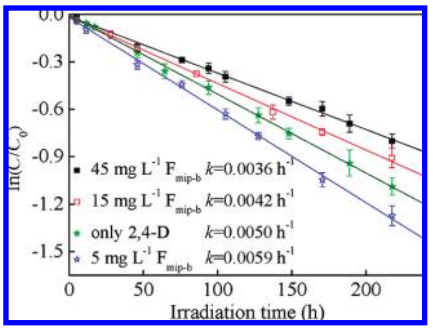

Figure 5. First-order rate constants (k) calculated at different initial F_{mip-b} concentrations on 2,4-D (1 mg L^{-1}) degradation.

concentration at time t and C_0 is the initial concentration. The 2,4-D degradation rate constants in the presence of F_{mip-b}, F_{eff}, bulk HA, and only 2,4-D without any HA or its fractions were 0.0059, 0.0024, 0.0034, and 0.0050 h^{-1}, respectively. The rate constant for F_{mip-b} was 2.5 times that for F_{eff} and 1.7 times that for bulk HA. This result demonstrated dependence of photochemical activity on the structure of HA, and herein F_{mip-b}, which accounts for *Pc*-like structures, had better photochemical activity in inducing 2,4-D photodegradation.

The photodegradation of 2,4-D may proceed both via direct photodecomposition after absorption photons from light radiation and via an indirect process induced by ROS, which results from the interaction of sunlight and HA (*6*). It was observed that photochemical degradation of 2,4-D under the condition without any HA and its fractions was relatively fast in comparison with F_{eff} or bulk HA, although it was slower than F_{mip-b}. Figure S5 of the Supporting Information shows that 2,4-D displays two absorbance bands in the near-UV region. One is around 220−240 nm and the other, around 260−300 nm. It is possible that light with $\lambda > 290$ nm could induce direct photodegradation of 2,4-D. The reason for accelerated degradation of 2,4-D in the presence of F_{mip-b} could be that F_{mip-b} might produce more ROS under simulated solar light irradiation, which benefited 2,4-D degradation through ROS reaction approach. An EPR spin-trapping technique is an efficient method to determine short-lived ROS and is useful for understanding the photodegradation process (*25*). To further reveal the photodecomposition mechanism of 2,4-D in the presence of HA and its fractions under irradiation at $\lambda > 290$ nm, the peak intensities, which are related to the free radical concentrations, were recorded by EPR spectrometer. **Figure 4** illustrates the EPR spectra of the DMPO−OH• spin adduct with pulsed laser illumination at $\lambda = 355$ nm in the solutions of HA and its fractions (32 mg L^{-1}). In the dark (0 s), no signal could be detected. Under irradiation (80 s), the characteristic 1:2:2:1 quadruple peaks of the DMPO−OH• adduct were observed in the presence of HA and its fractions. This indicates that OH• radicals are generated (*26*) and can participate in the photoreaction at $\lambda > 290$ nm irradiation in solutions containing HA or its fractions. Furthermore, compared with F_{eff} and bulk HA, F_{mip-b} generated stronger DMPO−OH• signals, indicating that more hydroxyl radicals were generated in F_{mip-b} solution. For the systems with F_{eff} and bulk HA, due to the competition for photons between 2,4-D and F_{eff} or bulk HA, the direct photolysis of 2,4-D would be inhibited. In the presence of F_{eff} and bulk HA, the amount of OH• was not enough to compensate for the inhibition effect caused by the competition for photons, and as a consequence the photodegradation of 2,4-D was retarded. The result suggested that better photochemical activity of F_{mip-b} on 2,4-D degradation might contribute to effective oxidation of 2,4-D by ROS such as OH•.

Effects of Concentration of MIP Trapped Fraction on 2,4-D Photodegradation. Figure 5 shows the 2,4-D photodegradation (initially 1 mg L^{-1}) at initial F_{mip-b} concentrations of 5, 15, and 45 mg L^{-1}. It was interesting to note that at the lower concentration (5 mg L^{-1}) of F_{mip-b}, 2,4-D degradation was enhanced in comparison to that without any HA fraction, whereas it slowed as the concentration of F_{mip-b} increased. The 2,4-D degradation rate constants for solutions with 5, 15, and 45 mg L^{-1} of F_{mip-b} were 0.0059, 0.0042, and 0.0036 h^{-1}, respectively. The results could be principally attributed to a high capability for absorbing photons by F_{mip-b}, and the absorption increased with the increase of F_{mip-b} concentration (data not shown). At higher concentrations of F_{mip-b}, although it had a higher photochemical activity, the amount of OH• was not enough to compensate for the inhibition effect caused by the competition for photons, and as a consequence the direct photodegradation of 2,4-D was retarded. Bachman et al. (*27*) reported similar results that photodegradation of a carbamate pesticide, carbofuran, slowed with increasing DOM concentration. They postulated that the decrease in the rate of photodegradation of carbofuran could be due to DOM competing with carbofuran for available photons. In addition, the inhibition of DOM could be related to the binding interaction between DOM and PTS (*27*). When F_{mip-b} and 2,4-D coexisted in solution, the herbicide 2,4-D was possibly bound to F_{mip-b}. It was believed that the binding occurred predominantly through a hydrophobic partitioning mechanism (*28*), which drew the 2,4-D molecule into an aggregate of F_{mip-b} complex molecules. This allowed the 2,4-D molecule to transfer the excess energy resulting from the absorption of photons to the surrounding F_{mip-b} molecules, which promoted the photoreaction of F_{mip-b} but inhibited the photodegradation of 2,4-D. The study by Fu et al. (*28*) also supported the suggestion. As a result, a lower concentration of F_{mip-b} could accelerate 2,4-D photodegradation, and a higher concentration could inhibit the process; the retarded effect was increased with the increase of F_{mip-b} concentration.

The present work demonstrates the feasibility of separating HA according to structure speciation using MIP technique. This approach is helpful in better elucidating HA structures and further understanding the relationship between their structures and the photochemical fate of PTS in natural aquatic systems. Our results present the *Pc*-like structures of HA as having better photochemical activity and further indicated the dependence of HA photochemical activity on their structures, which could eventually affect photodegradation of other coexisting organic compounds. As a novel separation method, a MIP technique may be applied to probe for other structural moieties in HA in the future.

Supporting Information Available: Detailed information includes chemical structures of chlorophyll and phthalocyanine (Figure S1); molecular imprinting process and formation of hydrogen bonds between imprinting molecule (CuPc) and functional monomer (MAA) (Figure S2); UV−vis DRS spectra of imprinted polymers (MIP) and nonimprinted polymers (NIP) before and after binding (a) CuPc, and UV−vis spectra of original solutions and effluents through MIP and NIP for (b) oxalic acid, (c) citric acid, (d) salicylic acid, (e) glucose, and (f) sucrose (Figure S3); chemical structures of five molecules used to study the selectivity of MIP (Figure S4); and UV−vis spectra of 1 mg L^{-1} 2,4-D (Figure S5). This material is available free of charge via the Internet at http://pubs.acs.org.

LITERATURE CITED

(1) Walse, S. S.; Morgan, S. L.; Kong, L.; Ferry, J. L. Role of dissolved organic matter, nitrate, and bicarbonate in the photolysis of aqueous fipronil. *Environ. Sci. Technol.* **2004**, *38*, 3908–3915.

(2) Fisher, J. M.; Reese, J. G.; Pellechia, P. J.; Moeller, P. L.; Ferry, J. L. Role of Fe(III), phosphate, dissolved organic matter, and nitrate during the photodegradation of domoic acid in the marine environment. *Environ. Sci. Technol.* **2006**, *40*, 2200–2205.

(3) Ou, X. X.; Quan, X.; Chen, S.; Zhao, H. M.; Zhang, Y. B. Atrazine photodegradation in aqueous solution induced by interaction of humic acids and iron: photoformation of iron(II) and hydrogen peroxide. *J. Agric. Food Chem.* **2007**, *55*, 8650–8656.

(4) Aguer, J. P.; Richard, C.; Andreux, F. Comparison of the photoinductive properties of commercial, synthetic and soil-extracted humic substances. *J. Photochem. Photobiol. A* **1997**, *103*, 163–168.

(5) Chen, J.; Gu, B. H.; LeBoeuf, E. J.; Pan, H. J.; Dai, S. Spectroscopic characterization of the structural and functional properties of natural organic matter fractions. *Chemosphere* **2002**, *48*, 59–68.

(6) Ou, X. X.; Chen, S.; Quan, X.; Zhao, H. M. Photoinductive activity of humic acid fractions with the presence of Fe(III): the role of aromaticity and oxygen groups involved in fractions. *Chemosphere* **2008**, *72*, 925–931.

(7) Richard, C.; Trubetskaya, O.; Trubetskoj, O.; Reznikova, O.; Afanas'eva, G.; Aguer, J.-P.; Guyot, G. Key role of the low molecular size fraction of soil humic acids for fluorescence and photoinductive activity. *Environ. Sci. Technol.* **2004**, *38*, 2052–2057.

(8) Trubetskoj, O. A.; Trubetskaya, O. E.; Afanas'eva, G. V.; Reznikova, O. I.; Saiz-Jimenez, C. Polyacrylamide gel electrophoresis of soil humic acid fractionated by size-exclusion chromatography and ultrafiltration. *J. Chromatogr., A* **1997**, *767*, 285–292.

(9) Gao, D. M.; Zhang, Z. P.; Wu, M. H.; Xie, C. G.; Guan, G. J.; Wang, D. P. A surface functional monomer-directing strategy for highly dense imprinting of TNT at surface of silica nanoparticles. *J. Am. Chem. Soc.* **2007**, *129*, 7859–7866.

(10) Yilmaz, E.; Haupt, K.; Mosbach, K. The use of immobilized templates—a new approach in molecular imprinting. *Angew. Chem., Int. Ed.* **2000**, *39*, 2115–2118.

(11) Alexander, C.; Davidson, L.; Hayes, W. Imprinted polymers: artificial molecular recognition materials with applications in synthesis and catalysis. *Tetrahedron* **2003**, *59*, 2025–2057.

(12) Shen, X. T.; Zhu, L. H.; Li, J.; Tang, H. Q. Synthesis of molecular imprinted polymer coated photocatalysts with high selectivity. *Chem. Commun.* **2007**, 1163–1165.

(13) Heaton, J. W.; Lencki, R. W.; Marangoni, A. G. Kinetic model for chlorophyll degradation in green tissue. *J. Agric. Food Chem.* **1996**, *44*, 399–402.

(14) Liu, Y. H.; Lei, S. B.; Yin, S. X.; Xu, S. L.; Zheng, Q. Y.; Zeng, Q. D.; Wang, C.; Wan, L. J.; Bai, C. L. Molecular trapping phenomenon of the 2-D assemblies of octa-alkoxyl-substituted phthalocyanine studied by scanning tunneling microscopy. *J. Phys. Chem. B* **2002**, *106*, 12569–12574.

(15) Karan, S.; Mallik, B. Templating effects and optical characterization of copper(II) phthalocyanine nanocrystallites thin film: nanoparticles, nanoflowers, nanocabbages, and nanoribbons. *J. Phys. Chem. C* **2007**, *111*, 7352–7365.

(16) Lawton, E. A. The thermal stability of copper phthalocyanine. *J. Phys. Chem.* **1958**, *62*, 384–384.

(17) Xing, S. T.; Hu, C.; Qu, J. H.; He, H.; Yang, M. Characterization and reactivity of MnO_x supported on mesoporous zirconia for herbicide 2,4-D mineralization with ozone. *Environ. Sci. Technol.* **2008**, *42*, 3363–3368.

(18) Sutherland, D. J.; Stearman, G. K.; Wells, M. J. M. Development of an analytical scheme for simazine and 2,4-D in soil and water runoff from ornamental plant nursery plots. *J. Agric. Food Chem.* **2003**, *51*, 14–20.

(19) Chizhov, I.; Scoles, G.; Kahn, A. The influence of steps on the orientation of copper phthalocyanine monolayers on Au(111). *Langmuir* **2000**, *16*, 4358–4361.

(20) Almendros, G.; Kgathi, D.; Sekhwela, M.; Zancada, M.-C.; Tinoco, P.; Pardo, M.-T. Biogeochemical assessment of resilient humus formations from virgin and cultivated northern Botswana soils. *J. Agric. Food Chem.* **2003**, *51*, 4321–4330.

(21) Peuravuori, J.; Pihlaja, K. Preliminary study of lake dissolved organic matter in light of nanoscale supramolecular assembly. *Environ. Sci. Technol.* **2004**, *38*, 5958–5967.

(22) Pullin, M. J.; Cabaniss, S. E. Rank analysis of the pH-dependent synchronous fluorescence spectra of six standard humic substances. *Environ. Sci. Technol.* **1995**, *29*, 1460–1467.

(23) Yamashita, Y.; Jaffé, R. Characterizing the interactions between trace metals and dissolved organic matter using excitation-emission matrix and parallel factor analysis. *Environ. Sci. Technol.* **2008**, *42*, 7374–7379.

(24) Fukushima, M.; Tanaka, S.; Nakamura, H.; Ito, S.; Haraguchi, K.; Ogata, T. Copper(II) binding abilities of molecular weight fractionated humic acids and their mixtures. *Anal. Chim. Acta* **1996**, *322*, 173–185.

(25) Chang, Q. Y.; He, H.; Zhao, J. C.; Yang, M.; Qu, J. H. Bactericidal activity of a Ce-promoted $Ag/AlPO_4$ catalyst using molecular oxygen in water. *Environ. Sci. Technol.* **2008**, *42*, 1699–1704.

(26) Yu, J. C.; Ho, W. K.; Yu, J. G.; Yip, H.; Wong, P. K.; Zhao, J. C. Efficient visible-light-induced photocatalytic disinfection on sulfur-doped nanocrystalline titania. *Environ. Sci. Technol.* **2005**, *39*, 1175–1179.

(27) Bachman, J.; Patterson, H. H. Photodecomposition of the carbamate pesticide carbofuran: Kinetics and the influence of dissolved organic matter. *Environ. Sci. Technol.* **1999**, *33*, 874–881.

(28) Fu, H. B.; Quan, X.; Liu, Z. Y.; Chen, S. Photoinduced transformation of γ-HCH in the presence of dissolved organic matter and enhanced photoreactive activity of humate-coated α-Fe_2O_3. *Langmuir* **2004**, *20*, 4867–4873.

Received May 17, 2009. Revised manuscript received June 30, 2009. Accepted June 30, 2009. The work was supported by the National Basic Research Program of China (No. 2004CB418504 and 2007CB407302) and the National Science Fund for Distinguished Young Scholars of China (No. 20525723).